

The Hong-Ou-Mandel effect in the context of few-photon scattering

Paolo Longo,^{1,*} Jared H. Cole,² and Kurt Busch³

¹*Institut für Theoretische Festkörperphysik, Karlsruher Institut für Technologie (KIT), 76131 Karlsruhe, Germany*

²*Chemical and Quantum Physics, School of Applied Sciences, RMIT University, Melbourne 3001, Australia*

³*Humboldt-Universität zu Berlin, Institut für Physik, AG Theoretische Optik & Photonik, Newtonstr. 15, 12489 Berlin, and Max-Born-Institut, Max-Born-Str. 2A, 12489 Berlin, Germany*

[*paolo.longo@kit.edu](mailto:paolo.longo@kit.edu)

Abstract: The Hong-Ou-Mandel effect is studied in the context of two-photon transport in a one-dimensional waveguide with a single scatterer. We numerically investigate the scattering problem within a time-dependent, wave-function-based framework. Depending on the realization of the scatterer and its properties, we calculate the joint probability of finding both photons on either side of the waveguide after scattering. We specifically point out how Hong-Ou-Mandel interferometry techniques could be exploited to identify effective photon-photon interactions which are mediated by the scatterer. The Hong-Ou-Mandel dip is discussed in detail for the case of a single two-level atom embedded in the waveguide, and dissipation and dephasing are taken into account by means of a quantum jump approach.

© 2012 Optical Society of America

OCIS codes: (270.0270) Quantum optics; (290.0290) Scattering.

References and links

1. C. K. Hong, Z. Y. Ou, and L. Mandel, "Measurement of subpicosecond time intervals between two photons by interference," *Phys. Rev. Lett.* **59**, 2044–2046 (1987).
2. Y. L. Lim and A. Beige, "Generalized Hong-Ou-Mandel experiments with bosons and fermions," *New J. Phys.* **7**, 155 (2005).
3. V. Giovannetti, D. Frustaglia, F. Taddei, and R. Fazio, "Electronic Hong-Ou-Mandel interferometer for multi-mode entanglement detection," *Phys. Rev. B* **74**, 115315 (2006).
4. I. A. Walmsley and M. G. Raymer, "Toward quantum-information processing with photons," *Science* **307**, 1733–1734 (2005).
5. H. Takesue, "1.5 μm band Hong-Ou-Mandel experiment using photon pairs generated in two independent dispersion shifted fibers," *Appl. Phys. Lett.* **90**, 204101 (2007).
6. A. Peruzzo, A. Laing, A. Politi, T. Rudolph, and J. L. O'Brien, "Multimode quantum interference of photons in multipoint integrated devices," *Nat. Commun.* **2**, 224 (2011).
7. S. M. Wang, S. Y. Mu, C. Zhu, X. Y. Gong, P. Xu, H. Liu, T. Li, S. N. Zhu, X. Zhang, "Hong-Ou-Mandel interference mediated by the magnetic plasmon waves in a three-dimensional optical metamaterial," *Opt. Express* **20**, 5213–5218 (2012).
8. P. Longo, P. Schmitteckert, and K. Busch, "Dynamics of photon transport through quantum impurities in dispersion-engineered one-dimensional systems," *J. Opt. A: Pure Appl. Opt.* **11**, 114009 (2009).
9. P. Longo, P. Schmitteckert, and K. Busch, "Few-photon transport in low-dimensional systems," *Phys. Rev. A* **83**, 063828 (2011).
10. C. G. Gerry and P. L. Knight, *Introductory Quantum Optics* (Cambridge University Press, 2005).
11. Z. Y. Ou, C. K. Hong, L. Mandel, "Relation between input and output states for a beam splitter," *Opt. Commun.* **63**, 118–122 (1987).

12. A. Yariv, Y. Xu, R. K. Lee, and A. Scherer, "Coupled-resonator optical waveguide: a proposal and analysis," *Opt. Lett.* **24**, 711–713 (1999).
13. L. Zhou, Z. R. Gong, Y. X. Liu, C. P. Sun, and F. Nori, "Controllable scattering of a single photon inside a one-dimensional resonator waveguide," *Phys. Rev. Lett.* **101**, 100501 (2008).
14. P. Longo, P. Schmitteckert, and K. Busch, "Few-photon transport in low-dimensional systems: interaction-induced radiation trapping," *Phys. Rev. Lett.* **104**, 023602 (2010).
15. J. T. Shen and S. Fan, "Coherent photon transport from spontaneous emission in one-dimensional waveguides," *Opt. Lett.* **30**, 2001–2003 (2005).
16. E. Rephaeli, J. T. Shen, and S. Fan, "Full inversion of a two-level atom with a single-photon pulse in one-dimensional geometries," *Phys. Rev. A* **82**, 033804 (2010).
17. J. T. Shen and S. Fan, "Theory of single-photon transport in a single-mode waveguide. I. Coupling to a cavity containing a two-level atom," *Phys. Rev. A* **79**, 023837 (2009).
18. J. T. Shen and S. Fan, "Strongly correlated two-photon transport in a one-dimensional waveguide coupled to a two-level system," *Phys. Rev. Lett.* **98**, 153003 (2007).
19. J. T. Shen and S. Fan, "Strongly correlated multi-particle transport in one dimension through a quantum impurity," *Phys. Rev. A* **76**, 062709 (2007).
20. T. Shi and C. P. Sun, "Lehmann-Symanzik-Zimmermann reduction approach to multiphoton scattering in coupled resonator arrays," *Phys. Rev. B* **79**, 205111 (2009).
21. D. Witthaut and A. S. Sørensen, "Photon scattering by a three-level emitter in a one-dimensional waveguide," *New J. Phys.* **12**, 043052 (2009).
22. M. B. Plenio and P. L. Knight, "The quantum-jump approach to dissipative dynamics in quantum optics," *Rev. Mod. Phys.* **70**, 101–144 (1998).
23. K. Mølmer, Y. Castin, and J. Dalibard, "Monte Carlo wave-function method in quantum optics," *J. Opt. Soc. Am. B* **10**, 524–538 (1993).
24. Y. Saad, "Analysis of some Krylov subspace approximations to the matrix exponential operator," *SIAM Journal on Numerical Analysis* **29**, 209–228 (1992).
25. J. Niegemann, L. Tkeshelashvili, and K. Busch, "Higher-order time-domain simulations of Maxwell's equations using Krylov-subspace methods," *J. Comput. Theor. Nanosci.* **4**, 627–634 (2007).
26. M. Pototschnig, J. Niegemann, L. Tkeshelashvili, and K. Busch, "Time-domain simulation of the nonlinear Maxwell equations using operator-exponential techniques," *IEEE Trans. Ant. Propagat.* **57**, 475–483 (2009).
27. K. Busch, G. v. Freymann, S. Linden, S. F. Mingaleev, L. Tkeshelashvili, and M. Wegener, "Periodic nanostructures for photonics," *Phys. Rep.* **444**, 101–202 (2007).
28. M. J. Hartmann, F. G. S. L. Brandao, and M. B. Plenio, "Strongly interacting polaritons in coupled arrays of cavities," *Nat. Phys.* **2**, 849–855 (2006).
29. A. Greentree, C. Tahan, J. Cole, and L. Hollenberg, "Quantum phase transitions of light," *Nat. Phys.* **2**, 856–861 (2006).
30. D. Angelakis, M. Santos, S. Bose, "Photon-blockade-induced Mott transitions and XY spin models in coupled cavity arrays," *Phys. Rev. A* **76**, 31805 (2007).
31. M. I. Makin, J. H. Cole, C. D. Hill, A. D. Greentree, and L. C. L. Hollenberg, "Time evolution of the one-dimensional Jaynes-Cummings-Hubbard Hamiltonian," *Phys. Rev. A* **80**, 043842 (2009).
32. J. Q. Quach, C.-H. Su, A. M. Martin, A. D. Greentree, and L. C. L. Hollenberg, "Reconfigurable quantum metamaterials," *Opt. Express* **19**, 11018–11033 (2011).
33. M. T. C. Wong and C. K. Law, "Two-polariton bound states in the Jaynes-Cummings-Hubbard model," *Phys. Rev. A* **83**, 055802 (2011).
34. D. E. Chang, A. S. Sørensen, E. A. Demler, and M. D. Lukin, "A single-photon transistor using nanoscale surface plasmons," *Nat. Phys.* **3**, 807–812 (2007).
35. M. A. Noginov, G. Zhu, A. M. Belgrave, R. Bakker, V. M. Shalaev, E. E. Narimanov, S. Stout, E. Herz, T. Suteewong, and U. Wiesner, "Demonstration of a spaser-based nanolaser," *Nature* **460**, 1110–1112 (2009).
36. R. Yan, P. Pausauskie, J. Huang, and P. Yang, "Direct photonic-plasmonic coupling and routing in single nanowires," *Proc. Natl. Acad. Sci. USA* **106**, 21045–21050 (2009).

1. Introduction

Two photons impinging on a balanced beam splitter from different ports leave the device together in either one of the two output ports. This rather counter-intuitive and inherently quantum mechanical phenomenon, which is known as the Hong-Ou-Mandel effect, was demonstrated experimentally in 1987 [1]. Since then, the topic of two-photon interference turned into a rich and multifaceted field of research. Besides the generalization of the Hong-Ou-Mandel effect to the multi-particle case [2] or the proposal of its fermionic analog [3], it is believed that Hong-Ou-Mandel interference can be successfully exploited in the context of linear-optical quantum

computation [4]. Indeed, since photons themselves rarely interact with each other, they seem to be difficult to manipulate and process. The Hong-Ou-Mandel effect, however, solely relies on the statistics of the involved particles and is therefore at the very heart of quantum optics *per se*. To date, photon pairs can be routinely sent through optical fibers [5], and—due to the rapid progress in the fabrications of nano-photon components—integrated optical waveguiding structures on silicon chips are very promising candidates towards more complicated networks of multimode interference devices [6]. Furthermore, in the realm of optical metamaterials, the measurement of the Hong-Ou-Mandel dip for magnetic plasmon waves has been reported recently [7].

Of course, these examples only represent a very incomplete and biased selection from the vast amount of publications available on this topic and a well-balanced review of all relevant works is clearly beyond the scope of this paper. However, the beam splitter in a Hong-Ou-Mandel setup is very often just regarded as an optical component with which one can study the quantum mechanical nature of light by means of coincidence experiments. In this paper, we take a slightly different viewpoint and address the question of how the Hong-Ou-Mandel effect can be exploited—used as a probe—to learn something about the properties of the beam-splitting device itself. This question is of direct relevance to the problem of two photons propagating from different ends in a waveguide towards a scatterer, e.g., an artificial atom. We therefore numerically investigate such a scattering problem in a time-dependent, wave-function-based formalism [8, 9].

The outline of this paper is as follows. In Sec. 2, we start by reviewing the quantum mechanical description of a beam splitter, the Hong-Ou-Mandel effect, and its relation to scattering problems. After a qualitative motivation for why the Hong-Ou-Mandel effect can serve as a probe for effective photon–photon interactions, we introduce the types of scatterers which are investigated in this paper, i.e., a local on-site potential and a two-level atom. We formulate the corresponding Hamiltonians with regard to a one-dimensional tight-binding waveguide and present the beam-splitter conditions which are deduced from the stationary single-particle scattering states. The numerical framework is explained in Sec. 3 and the central quantity of this paper—the joint probability of finding both photons on either side of the waveguide after scattering—is defined. In Sec. 4, we provide a detailed analysis of the Hong-Ou-Mandel dip for the case of a local on-site potential and a two-level atom. Since the latter is a saturable absorber, effective photon–photon interactions are important. In addition, we take dissipation of T_1 -type and dephasing of T_2 -type into account. We conclude the paper in Sec. 5 and give a short outlook on possible future work.

2. Fundamentals

2.1. The quantum-mechanical beam splitter as a four-port device and its relation to scattering problems

A consistent quantum-mechanical treatment of a beam splitter requires its interpretation as a four-port device [1, 10, 11]. Since the “usual” type of beam splitter does not induce direct interactions between the involved particles—in the majority of cases photons—its single-particle solution can be readily applied to the multi-particle case. With the help of the scattering matrix formalism, the operators for the input ports 0 and 1 (a_0 and a_1) can be related to the output ports 2 and 3 (operators a_2 and a_3 , cf. Fig. 1). The transformation reads

$$\begin{pmatrix} a_2 \\ a_3 \end{pmatrix} = \hat{S} \begin{pmatrix} a_0 \\ a_1 \end{pmatrix}, \quad (1)$$

where

$$\hat{S} = \begin{pmatrix} t' & r \\ r' & t \end{pmatrix} \quad (2)$$

represents the scattering matrix with the corresponding reflection and transmission amplitudes (cf. Ref. [10]). Note that up to this point no statement about the commutation and anticommutation relations of the operators involved is required. This formalism is valid both for bosons and fermions. The reciprocity relations and the conservation of the total probability can be deduced by enforcing the same particle statistics for the operators describing the in- and output ports (cf. Eq. (1)).

The general form of the scattering matrix above allows for a description of unbalanced beam splitters which do not equally “split” a single photon into the two output ports. However, the effect we aim at in the following—the Hong-Ou-Mandel effect—can be best understood for the case where the beam splitter is balanced, i.e., a single particle scattering off the beam splitter will be in one of the output arms with equal probability of 50%.

For simplicity, we restrict ourselves to the case of photons here. The reflected beam undergoes a phase shift of $\pi/2$ and we thus have $t' = t = 1/\sqrt{2}$ and $r = r' = i/\sqrt{2}$ [10]. Next, we consider an input state with two photons in different input ports, i.e.,

$$|\text{in}\rangle = a_0^\dagger a_1^\dagger |0\rangle, \quad (3)$$

where $|0\rangle$ represents the vacuum state. According to Eqs. (1) and (2), the corresponding output state is

$$\begin{aligned} |\text{out}\rangle &= \frac{1}{2} (a_2^\dagger + ia_3^\dagger) (ia_2^\dagger + a_3^\dagger) |0\rangle \\ &= \frac{i}{2} (a_2^\dagger a_2^\dagger + a_3^\dagger a_3^\dagger) |0\rangle. \end{aligned} \quad (4)$$

This remarkable result, which is known as the Hong-Ou-Mandel effect [1], states that two photons impinging on a beam splitter from different input ports leave the device “together” in either one of the output ports. For a balanced beam splitter, the probability of finding one photon in one output arm and the other photon in the other arm is zero. The Hong-Ou-Mandel effect is a true quantum mechanical effect in the sense that it cannot be obtained in the limit of a low-intensity coherent state (cf. Ref. [10]). The tendency of photons to “stick together” is a consequence of the bosonic particle statistics. Fermions behave the opposite way, i.e., the probability of finding two fermions in one output arm is zero.

In experiments, one usually faces photonic wave packets of finite width. The initial difference in the distance of both wave packets to the beam splitter determines their overlap at the position of the beam splitter and thus influences the joint probability of both particles leaving the device in the same port. The joint probability of both photons leaving the device in different ports, which can be obtained from coincidence measurements, shows a dip as a function of the difference in the separation to the beam splitter. This dip is known as the “Hong-Ou-Mandel dip” and was first reported in 1987 [1].

Now, we establish a connection between the beam splitter as a four-port device and the scattering of photons at a local impurity. In scattering theory, one usually divides the system into left and right leads, e.g., a waveguide in the context of photons, and a local scattering potential which is placed in the middle. By means of the scattering matrix formalism, a single-particle input state $|\text{in}\rangle = |k\rangle = a_k^\dagger |0\rangle$ of momentum k is transformed into a transmitted and a reflected momentum state according to $|\text{out}\rangle = \hat{S}|\text{in}\rangle$ with

$$a_k^\dagger \rightarrow \hat{S}a_k^\dagger = r_k a_{-k}^\dagger + t_k a_k^\dagger \quad (5)$$

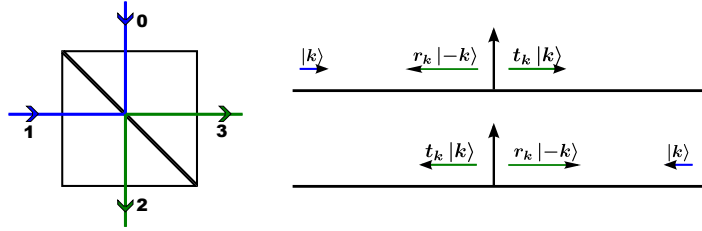


Fig. 1. Schematic sketch of a beam splitter as a four-port device and its analogy to a scattering problem.

where r_k and t_k signify the reflection and transmission amplitudes, respectively. For an in-state in the left lead, we need to demand $k > 0$, for the right lead $k < 0$. We thus have 4 “ports” in total, namely $k > 0$ and $k < 0$ for the left and the right lead, respectively (cf. Fig. 1). We assume the magnitude of the momentum, $|k|$, to be unchanged here. In other words, we assume the single-particle scattering process to be elastic and the Hamiltonian to be time-reversal symmetric.

The analogy to the aforementioned balanced beam splitter is completed by demanding $|r_k|^2 = |t_k|^2 = \frac{1}{2}$ which—strictly speaking—can only be achieved for a single frequency since beam splitters are dispersive optical elements.

2.2. Hong-Ou-Mandel interferometry as a probe for photon–photon interactions

In many cases, the equations of motion for a single-photon state and a coherent state are identical or describe—at least approximately—the same dynamics in the low-intensity limit. Thus, although the equations for a single photon are deduced from the Schrödinger equation, they do not provide “more physics” than the corresponding equations for the coherent state. Of course, the evolution is always given by the Heisenberg equations of motion (or the Schrödinger equation), for either single-photon or coherent states. The differences comes about in the phase insensitivity of the single-photon state in contrast to the coherent state where the superposition of the various components of different photon number have a defined phase relationship with each other as well as an external phase reference. However, “true” quantum mechanical effects which go beyond interference effects in a wave mechanical sense mainly occur for two reasons.

First, the inherent statistics of the underlying fundamental excitations, e.g., fermions, bosons, spins, or polaritons as a mixture thereof, can cause such “true” quantum mechanical effects since the concept of the fundamental commutation and anticommutation relations does not exist for c-number fields. The Hong-Ou-Mandel effect is probably the most prominent example in this regard, even though it is often only referred to as a two-particle interference effect.

Second, interacting particles can lead to a strong modification of the many-body solution in contrast to the single particle case. The interactions might be either direct such as the Coulomb interaction of electrons or effectively mediated, e.g., an effective photon–photon interaction induced by a saturable absorber.

In Sec. 4, we demonstrate how the Hong-Ou-Mandel effect serves as a probe for identifying effective photon–photon interactions. Influencing variables are selectively taken into account to study their effects on the shape of the Hong-Ou-Mandel dip which we obtain from the solution of the time-dependent problem.

2.3. Types of impurities and their single-particle scattering solution

2.3.1. General form of the scattering equation

For the remainder of this discussion, the leads of the system are modeled as a one-dimensional tight-binding waveguide with Hamiltonian $H_{\text{leads}} = \sum_x \left(\hbar\omega a_x^\dagger a_x - J(a_{x+1}^\dagger a_x + a_x^\dagger a_{x+1}) \right)$ and the local impurity couples to site x_0 . This Hamiltonian describes a chain of identical and equally spaced coupled optical resonators which form a waveguide whose dispersion relation is centered around the resonators' resonance frequency ω . Such a system could, for instance, be realized by appropriately placed micro-disk resonators. In that case, the nearest-neighbor hopping constant J is defined as the overlap integral of the electromagnetic field modes of adjacent resonators [12]. Besides the realization in the field of cavity arrays, the Hamiltonian can be used to approximately describe photon propagation in an optical fiber. Then, the quantity J is chosen such that the fibers dispersion relation is well-described around a certain operating wavelength of interest. Similar to Ref. [13], the single-particle scattering solution is obtained by solving the eigenvalue problem in the single-excitation subspace using the ansatz

$$\varphi_x = \begin{cases} e^{ikx} + r_k e^{-ikx} & x < x_0 \\ t_k e^{ikx} & x \geq x_0 \end{cases} \quad (6)$$

for the wave function amplitudes in the waveguide. The discrete scattering equation has the generic form

$$0 = (\hbar\omega - E)\varphi_x - J(\varphi_{x+1} + \varphi_{x-1}) + \delta_{xx_0} G(E)\varphi_{x_0} \quad (7)$$

where $E = \varepsilon_k = \omega - 2J\cos(ka)$ is the eigenenergy corresponding to wavenumber $k \in [-\pi/a, \pi/a]$ (for lattice constant a). The reflection amplitude is

$$r_k = -e^{-2ik} \frac{J^2 - (\hbar\omega - E + G(E) - Je^{ik})(\hbar\omega - E - Je^{-ik})}{J^2 - (\hbar\omega - E + G(E) - Je^{ik})(\hbar\omega - E - Je^{-ik})}. \quad (8)$$

The function $G(E)$ depends on the actual realization of the impurity. Note that $1 + r_k = t_k$ and the conservation of probability, $|r_k|^2 + |t_k|^2 = 1$, hold. We choose the zero of the energy of the free waveguide to lie in the middle of the cosine band, i.e., we set $\omega = 0$ in the following.

2.3.2. Local on-site potential

A local on-site potential can be regarded as a deviation of the eigenfrequency of one of the cavities forming the tight-binding waveguide. In that case, the total Hamiltonian reads $H = H_{\text{leads}} + H_{\text{pot}}$, where

$$H_{\text{pot}} = g a_0^\dagger a_0 \quad (9)$$

is the contribution due to the impurity, which is part of the tight-binding chain itself and g is the strength of the local on-site potential (cf. Fig. 2).

The function $G(E)$ then simply becomes (cf. Eq. (7))

$$G(E) = g. \quad (10)$$

Consequently, the reflection amplitude takes the form

$$r_k = -\frac{g}{g - 2iJ\sin(ka)}. \quad (11)$$

Thus, the balanced beam splitter with $|r_k|^2 = |t_k|^2 = \frac{1}{2}$ is realized for

$$g = \pm 2|J| |\sin(ka)|. \quad (12)$$

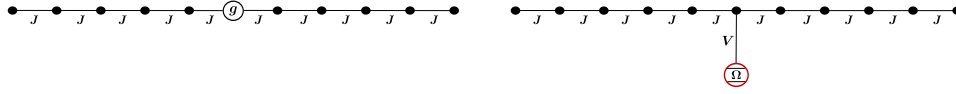


Fig. 2. Schematic sketch of a local on-site potential (left panel) and a two-level atom (right panel) in a tight-binding waveguide.

2.3.3. Local two-level system

A single two-level system coupled to the light modes of a tight-binding waveguide as well as various extensions thereof were discussed recently in different contexts [8, 9, 13–21]. The Hamiltonian takes the form of a single spin- $\frac{1}{2}$ locally side-coupled to a tight-binding waveguide, i.e., $H = H_{\text{leads}} + H_{\text{TLS}}$, where

$$H_{\text{TLS}} = \frac{\Omega}{2} \sigma_z + V \left(a_0^\dagger \sigma^- + a_0 \sigma^+ \right). \quad (13)$$

The transition energy of the two-level atom is denoted by Ω and V is the atom–cavity coupling strength (cf. Fig. 2).

The single-particle solution to this problem yields

$$G(E) = \frac{V^2}{E - \Omega} \quad (14)$$

and thus

$$r_k = \frac{V^2}{2iJ \sin(ka)(-\Omega - 2J \cos(ka)) - V^2}. \quad (15)$$

$|r_k|^2 = |t_k|^2 = \frac{1}{2}$ results in

$$V = \pm \sqrt{|2J \sin(ka)(-2J \cos(ka) - \Omega)|}. \quad (16)$$

For instance, $k = \frac{3\pi}{4a}$ yields $V = \pm \sqrt{\sqrt{2}|J| |\sqrt{2}J - \Omega|}$.

2.4. Influencing variables for the Hong-Ou-Mandel dip

In reality, various mechanisms lead to a fading of the Hong-Ou-Mandel dip. As mentioned before, wave packets have a finite width. Thus, the temporal overlap of two excitations at the position of the scatterer does not only depend on the difference in the initial distance to the latter but also on the widths of the wave packets. In realistic scenarios, single-particle excitations might experience a non-vanishing group velocity dispersion, which also influences the time of overlap at the position of the scatterer. Moreover, since the scattering solutions presented above are energy eigenstates, the “balanced beam splitter condition” can only be met for a single frequency out of the spectrum of the initial pulses.

From a theoretical point of view, it is interesting to monitor the qualitative change of the Hong-Ou-Mandel dip when the energy levels of the scatterer are smoothly changed from the harmonic to the strongly anharmonic case, i.e., when the transition from a harmonic oscillator to a two-level system is performed.

Additionally, in almost every realistic situation where atoms are coupled to light modes, dissipation and dephasing are important. The general form of a Lindblad master equation with a relaxation operator \hat{R} has the form $\partial_t \rho = \frac{i}{\hbar} [\rho, H] + \mathcal{L}(\rho)$, where ρ denotes the density matrix and the Lindbladian reads $\mathcal{L}(\rho) = \hat{R} \rho \hat{R}^\dagger - \frac{1}{2} \{ \hat{R}^\dagger \hat{R}, \rho \}$ (curly brackets denote an anti-commutator). In this formulation, dissipation of T_1 -type is described by the relaxation operator $\hat{R}_{T_1} = \sqrt{1/T_1} \sigma^-$. Dephasing of T_2 -type requires $\hat{R}_{T_2} = \sqrt{1/(2T_2)} \sigma_z$ [22, 23].

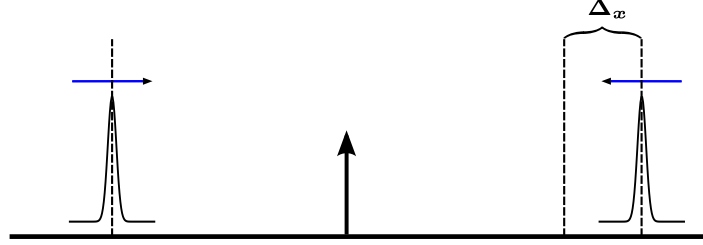


Fig. 3. Schematic sketch of the two-excitation initial state.

3. Time evolution, initial states, and physical quantities

In order to obtain the transport dynamics, we evolve quantum states in time according to

$$|\Psi(t)\rangle = e^{-\frac{i}{\hbar}Ht}|\Psi(0)\rangle, \quad (17)$$

where $|\Psi(t)\rangle$ stands for the state vector of radiation field and scatterer [8, 9, 14]. In the case of open quantum systems, i.e., if dissipation and dephasing are taken into account, a stochastic quantum jump formalism adapted from Refs. [22, 23] is applied. The deterministic part of the time evolution is carried out using Krylov-subspace-based operator-exponential techniques [24–26].

Since the Hong-Ou-Mandel effect requires a minimum of two excitations to be investigated, we choose our initial states to be of the form

$$|\Psi(0)\rangle = \sum_{x_1 x_2} \Phi_{x_1 x_2} a_{x_1}^\dagger a_{x_2}^\dagger |0\rangle, \quad (18)$$

where $\Phi_{x_1 x_2}$ is a boson-symmetric product of single-particle pulses launched from different ends of the waveguide (cf. Fig. 3). To be precise, the wave function is of the form

$$\Phi_{x_1 x_2} \propto \left(\begin{array}{l} \varphi_{x_1}^{k_0^{(1)} x_c^{(1)} s^{(1)}} \cdot \varphi_{x_2}^{k_0^{(2)} x_c^{(2)} s^{(2)}} \\ + \varphi_{x_2}^{k_0^{(1)} x_c^{(1)} s^{(1)}} \cdot \varphi_{x_1}^{k_0^{(2)} x_c^{(2)} s^{(2)}} \end{array} \right), \quad (19)$$

where $\varphi_x^{k_0 x_c s} \propto e^{\frac{(x-x_c)^2 a^2}{2s^2}} e^{ik_0 a x}$ is a Gaussian wave function with carrier wavenumber k_0 , center x_c , and width s . Unless stated otherwise, we choose $k_0^{(1)} = -k_0^{(2)} \equiv k_0 = \frac{3\pi}{4a}$, $s^{(1)} = s^{(2)} \equiv s = 7a$, $x_c^{(1)} \equiv x_c = 50$, and $x_c^{(2)} = N + 1 - x_c + \Delta_x/a$ in the following. Na is the total length of the waveguide. The relative displacement Δ_x is varied from $-30a$ to $+30a$ in order to record the Hong-Ou-Mandel dip. When $\Delta_x = 0$, both pulses initially have the same distance to the scatterer. The waveguide consists of $N = 199$ sites and the scatterer couples to site $x_0 = (N + 1)/2 = 100$. For the remainder, we take the nearest-neighbor hopping strength $J > 0$ as our fundamental energy scale. Consequently, time is measured in units of \hbar/J . Moreover, lengths are given in units of the lattice constant a so that carrier wave numbers have the unit $1/a$. We choose $\Delta t = 0.1\hbar/J$, which is smaller than any other time scale in the system, as the fundamental time step in the stochastic time evolution. For more information on the details of the simulation technique itself, we refer to Ref. [8].

With the knowledge of the two-excitation state vector $|\Psi(t)\rangle$ at all times, the calculation of arbitrary physical quantities becomes possible. According to Refs. [8, 9, 14], the time evolution of the occupation numbers $\langle a_x^\dagger a_x \rangle(t)$ allows us to monitor the motion of the wave packet in real

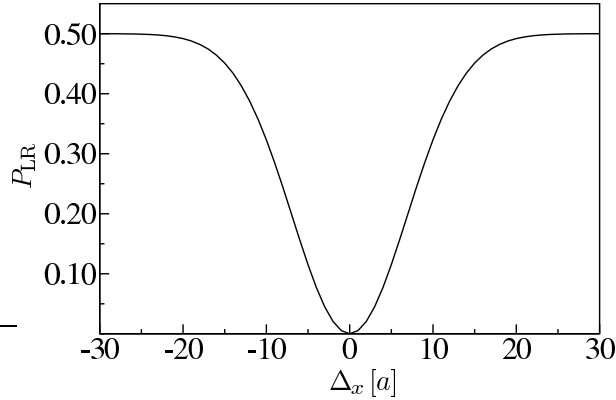


Fig. 4. Hong-Ou-Mandel dip for a system where a local scattering potential is coupled to a photonic tight-binding waveguide. The latter consists of $N = 199$ sites and the local scatterer in form of an on-site potential is coupled to site $x_0 = 100$. The strength of the potential is $g = 2|J|\sin(k_0a)$, which is the condition for a balanced beam splitter (cf. Eqs. (9) and (12)). We operate at a carrier wavenumber of $k_0 = \frac{\pi}{2a}$.

space. However, occupation numbers do not explicitly reveal correlations between the reflected and transmitted amounts of the two-excitation wave packet. Therefore, in order to obtain the Hong-Ou-Mandel dip, we define the quantity

$$P_{LR} = \frac{\sum_{\substack{x \in \mathcal{L} \\ y \in \mathcal{R}}} \langle a_y^\dagger a_x^\dagger a_x a_y \rangle}{\sum_{x,y \in \mathcal{L} \cup \mathcal{R}} \langle a_y^\dagger a_x^\dagger a_x a_y \rangle}, \quad (20)$$

which is the joint probability of finding one photon on the left ($\mathcal{L} = \{1, 2, \dots, x_0 - 1\}$) and the other on the right-hand side ($\mathcal{R} = \{x_0 + 1, \dots, N\}$) of the scatterer. Here, the site x_0 to which the scatterer is coupled is explicitly excluded from the summation since any excitation which might be trapped [14] either does not contribute to propagating modes or, for realistic systems, eventually decays into a loss channel in the long-time limit. Expression (20) has to be evaluated for times after the wave packets have scattered at the impurity but before the reflected and transmitted pulses are influenced by the system's hard-wall boundaries (for details we refer to Ref. [8]). Plotted as a function of Δ_x , i.e., as a function of the spatial separation of both incoming wave packets (cf. Fig. 3), Eq. (20) reproduces the famous Hong-Ou-Mandel dip.

4. Results and discussion

In this section, we present results on the numerical study of Hong-Ou-Mandel interferometry according to the setup as described above. We start with a scatterer in form of a local on-site potential. This setup resembles the situation of a “usual” beam splitter and results in a Hong-Ou-Mandel dip as originally reported in [1]. We then continue by replacing the local on-site potential with a two-level atom and gradually change its properties in order to study the resulting effects on the shape of the Hong-Ou-Mandel dip.

4.1. Local on-site potential in a tight-binding waveguide

In Fig. 4, we display the Hong-Ou-Mandel dip for a system as described in Sec. 2.3.2 and Eq. (9). We set $g = 2|J|\sin(k_0a)$ and operate at a carrier wavenumber of $k_0 = \frac{\pi}{2a}$. The coincidence probability of one photon being left and the other one being right practically vanishes

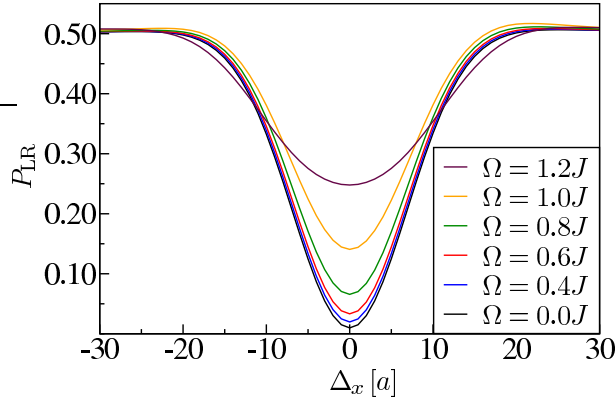


Fig. 5. Hong-Ou-Mandel dip for a system where a two-level system is coupled to a photonic tight-binding waveguide. For a central carrier wave number of $k_0 = \frac{3\pi}{4a}$, the beam splitter condition reads $V = \sqrt{\sqrt{2}|J| |\sqrt{2}J - \Omega|}$. Note that by varying the atomic transition energy relative to the cosine band, the atom-photon coupling strength V changes as well due to the beam splitter constraint. The combinations of transition energy and coupling strength used are $\Omega = 0: V = \sqrt{2}J$, $\Omega = 0.4J: V = 1.198J$, $\Omega = 0.6J: V = 1.073J$, $\Omega = 0.8J: V = 0.932J$, $\Omega = 1.0J: V = 0.765J$, $\Omega = 1.2J: V = 0.550J$.

for perfect overlap of the wave packets at the position of the scatterer, i.e., at $\Delta_x = 0$. For large separations, both wave packets pass the scatterer individually. Thus, one can read off the single-photon transmission probability at $\Delta_x \sim \pm 30a$ which is (nearly) perfect 50%. The reason why the local on-site potential works that well as a beam splitter for non-monochromatic excitations is because the reflectivity does not change for small deviations around the central carrier wavenumber of $k_0 = \frac{\pi}{2a}$, i.e., $\partial_k |r_k|^2|_{k=\pi/2a} = 0$ (not shown). This special property is due to a combination of the scatterer being part of the chain, i.e., it is not side-coupled, and the cosine dispersion of the tight-binding waveguide. Furthermore, effects due to non-linear dispersion are reduced since the group-velocity dispersion is zero at $k_0 = \frac{\pi}{2a}$.

4.2. Local two-level system in a tight-binding waveguide—the Hong-Ou-Mandel effect as a probe for photon–photon interactions

Now, we turn to the question of how a two-level system, which—in contrast to an on-site potential—is a saturable scatterer, qualitatively influences the Hong-Ou-Mandel dip. In the single-excitation subspace, there is no difference whether the atomic degree of freedom is treated as such or merely replaced by a bosonic site. However, two excitations can dramatically change the transport properties as was already demonstrated in the context of radiation trapping in Refs. [9, 14]. For this trapping effect to be most efficient, the photon energy should be on resonance with the atomic transition energy. This resonance condition cannot be fulfilled in the Hong-Ou-Mandel setup because the “balanced beam splitter condition” is required to achieve single-particle reflection and transmission with equal probability (cf. Eq. (16)). In the following, we choose $V = \sqrt{\sqrt{2}|J| |\sqrt{2}J - \Omega|}$ (cf. Sec. 2.3.3) and $k_0 = \frac{3\pi}{4a}$ (cf. Sec. 3).

4.2.1. Influence of the atomic transition energy on the Hong-Ou-Mandel dip

We start by varying the atomic transition energy Ω whilst keeping the beam splitter condition from Eq. (16). For instance, the Zeeman or Stark effect provide possible mechanisms of tuning

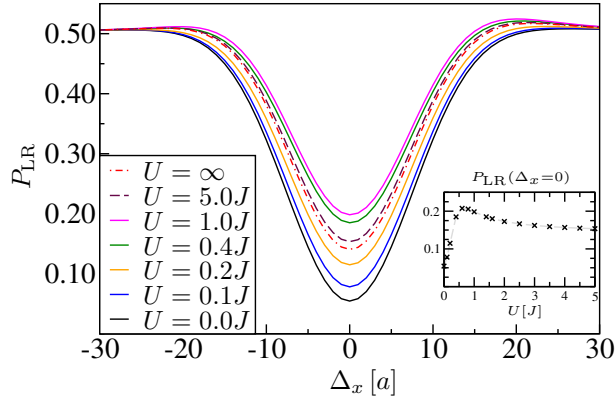


Fig. 6. Hong-Ou-Mandel dip for the same system as investigated in Fig. 5 but for $\Omega = J$ and different strengths of the anharmonicity U (see text for details). For $U = 0$, the fading of the Hong-Ou-Mandel dip is solely due to beam splitter imperfections at the single-photon level. The fading depends non-monotonically on the anharmonicity (see text for explanation). The single-photon limit ($\Delta \rightarrow \pm\infty$) is independent of the actual value of the anharmonicity. In the inset, we display the the depth of the Hong-Ou-Mandel dip as a function of the anharmonicity U (the gray line is just a guide to the eye).

the atomic transition energy. Increasing the atomic transition energy from $\Omega = 0$ to $\Omega = 1.2J$ has several consequences. First, the atom–photon detuning $\Omega - \varepsilon_{k=3\pi/4a} = \Omega - \sqrt{2}J$ is reduced. Second, the atom–photon coupling strength V is decreased. From Fig. 5 we can read off the tendency that the deviation from a perfect Hong-Ou-Mandel dip becomes more pronounced as the detuning is reduced. This is in line with Refs. [9, 14] because radiation trapping, which is one consequence of effective photon–photon interactions, is most efficient if $V \sim J$ and the resonance condition is fulfilled.

Mechanisms leading to such an effective photon–photon interaction can be identified in a faded Hong-Ou-Mandel dip. The fading is stronger than one would expect if only single-photon effects due to an unbalanced beam splitter were considered. This can be seen in Fig. 5 by noting that the limit of vanishing pulse overlap at the scatterer ($\Delta_x \rightarrow \pm\infty$) is nearly immune to changes in the atom–photon detuning. Since this limit represents individual particles passing the device, the fading of the Hong-Ou-Mandel dip must be due to effective photon–photon interactions whose effects can—at least in theory—be separated from signatures which are only induced by beam splitter imperfections.

The latter results in not all curves in Fig. 5 meeting exactly at $P_{LR} = 0.5$. The two-level atom acts as a dispersive beam splitter and—in contrast to the on-site potential—the atomic degree of freedom is side-coupled. Additionally, we operate in the non-linear regime of the dispersion relation ($k_0 = \frac{3\pi}{4a}$). Thus, the reflectivity does change to first order in small deviations around $k_0 = \frac{3\pi}{4a}$, i.e., $\partial_k |r_k|^2|_{k=3\pi/4a} \neq 0$ (not shown). As an example, we chose $\Omega = J$ in all subsequent considerations.

4.2.2. From the harmonic oscillator to the two-level system

From a theoretical point of view, the transition from a harmonic oscillator to a two-level system, i.e., from the harmonic to the strongly anharmonic case is most elucidating. In line with Refs. [9, 14], we therefore replace the Pauli operators of the two-level system in Eq. (13) by bosonic operators b and b^\dagger . Specifically, the formulation $\frac{\Omega}{2}\sigma_z \rightarrow \Omega b^\dagger b + U b^\dagger b (b^\dagger b - 1)$ describes a harmonic oscillator for $U = 0$ and a two-level system in the limit $U \rightarrow \infty$.

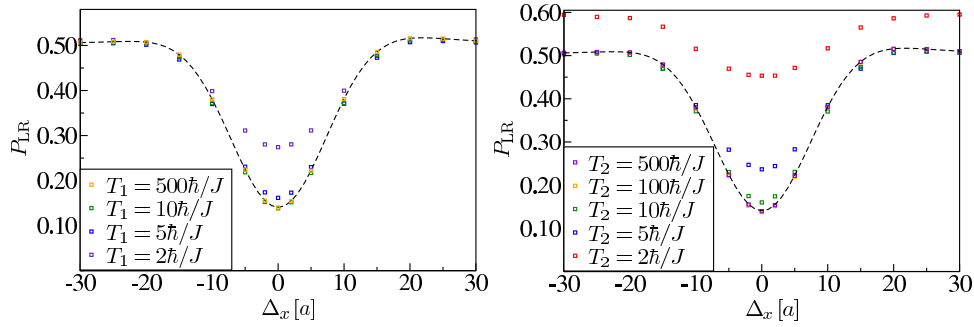


Fig. 7. Left panel: Hong-Ou-Mandel dip for the same parameters as in Fig. 5 with $\Omega = J$ but the two-level system experiences losses of T_1 -type. Even though losses of T_1 -type lead to irreversible photon loss, the single-photon limit is independent of the value of T_1 because of the normalization of Eq. (20). The black dashed curve represents the lossless case in which $T_1 = \infty$. We used 500 samples in the simulation for the stochastic time evolution. Right panel: Influence of pure dephasing of T_2 -type on the Hong-Ou-Mandel dip. Moderate dephasing times affect the depth of the Hong-Ou-Mandel dip but leave the single-photon limit practically unchanged. Very short dephasing times change the single-particle transport characteristics and, therefore, the single-photon limit in the Hong-Ou-Mandel dip. The black dashed curve represents the lossless case in which $T_2 = \infty$. We used 2000 samples in the simulation for the stochastic time evolution.

In Fig. 6, we display the Hong-Ou-Mandel dip for different strengths of the anharmonicity U . In the absence of interaction ($U = 0$), the Hong-Ou-Mandel dip becomes “perfect” besides the beam splitter imperfections due to the single-excitation transport characteristics. For $U > 0$, i.e., in the interacting system, the fading of the Hong-Ou-Mandel dip depends non-monotonically on the value of the anharmonicity until it saturates in the limit $U \rightarrow \infty$.

This behavior can be understood as follows. As demonstrated in Refs. [9, 14], the interactions induced by a finite U -term become most pronounced if the atom–photon detuning is zero. However, in the Hong-Ou-Mandel setup, the resonance condition is not fulfilled since the scatterer acts as a beam splitter. To further understand this non-monotonicity, it is helpful to consider the detuning between two impinging photons and the energy they had in case they double-occupied the atomic site, i.e., $\delta = n\Omega + Un(n-1) - n\varepsilon_{k_0}$, where $n = 2$ and ε_{k_0} is the single-photon energy. If the single-particle resonance condition, i.e., $\Omega = \varepsilon_{k_0}$, was fulfilled, δ would grow monotonically as U is increased. In the Hong-Ou-Mandel dip in Fig. 6, $\Omega - \varepsilon_{k_0} = (1 - \sqrt{2})J < 0$ so that δ changes its sign as U grows. This eventually leads to the non-monotonic dependence of the depth of the Hong-Ou-Mandel dip.

Note again that the offset in Fig. 6 in the limit of $\Delta \rightarrow \pm\infty$ is independent of the actual value of the anharmonicity. In this limit, the excitations pass the device individually as single particles.

4.2.3. Influence of dissipation and dephasing

In reality, even if the waveguide is considered to be practically lossless, the two-level system still suffers from non-radiative losses and the coupling to non-guided modes (subsumed in time constant T_1) as well as from pure dephasing, i.e., the randomization of the phase relation between the atom’s ground and excited state, (subsumed in time constant T_2).

In Fig. 7, we study the effect of different T_1 -times on the shape of the Hong-Ou-Mandel dip. Once a photon is lost, i.e., the T_1 -relaxation operator was applied to the two-particle state (cf. Sec. 2.4), the wave function collapses to a single-particle state and two-particle coincidences

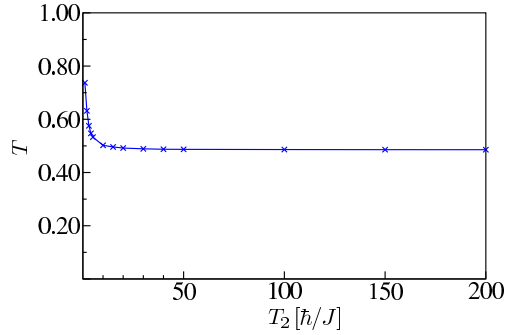


Fig. 8. Single-particle transmittance T through a two-level system which is subjected to pure dephasing of T_2 -type. For strong dephasing, i.e., T_2 -times comparable to the temporal overlap of the wavepacket at the position of the atom, the transmission is, for parameters we chose here, enhanced. We used $k_0 = \frac{3\pi}{4a}$, $s = 12a$, and $x_c = 50$ as parameters for the initial wave packet and 1000 samples in the simulation for the stochastic time evolution. The transmittance is defined in line with Ref. [8]. The solid line is just a guide to the eye.

become impossible, which leads to a less pronounced Hong-Ou-Mandel dip. However, since the definition of the joint probability P_{LR} in Eq. (20) is normalized to the total probability, the single-photon limit is independent of the value of T_1 . Note that in the quantum jump approach as described in Refs. [22, 23], all wave function trajectories enter the expectation values in Eq. (20), including those that represent zero coincidences.

The effect of pure dephasing on the Hong-Ou-Mandel dip is displayed in Fig. 7. The two-level atom mediates the effective photon-photon interaction less efficiently once the phase coherence between the atom and the impinging photons is destroyed. This leads to a fading of the Hong-Ou-Mandel dip but for moderate T_2 -times the single-photon limit seems to be practically unaffected. Only very short dephasing times lead to a significant change in the single-photon transport which results in the beam splitter being unbalanced and thus the single-photon limit changes.

This can be understood as follows. Pure dephasing can be regarded as the temporal fluctuation of the atom's level spacing. In the regime of strong dephasing, the detuning between the instantaneous atomic transition energy and the photon energy according to the central carrier wavenumber of the wave packet thus strongly fluctuates. This, in turn, implies that the condition for equal reflection and transmission of a monochromatic wave is only fulfilled for very short instances of time. In the present setup, this enhances the transmittance of the single-excitation wave packet (see Fig. 8). The transmittance is defined as [8] $T = \frac{1}{2} \langle a_{x_0}^\dagger a_{x_0} \rangle + \sum_{x=x_0+1}^N \langle a_x^\dagger a_x \rangle$. For the parameters chosen here, T_2 -times comparable to the temporal overlap τ of the wave packet at the position of the atom lead to an enhanced transmission. As a crude estimate, $\tau \sim s/v_g$, where $v_g = 2aJ\hbar^{-1} \sin(k_0a)$ is the group velocity.

From the above investigations one might get the impression that a clear-cut separation of the influences of the open system dynamics (T_1 and T_2) and the actual interaction between two excitations is impossible and one still would have to speculate to which degree an imperfect Hong-Ou-Mandel dip really is the signature for effective photon-photon interactions. We would like to emphasize that the previous studies were driven by the explicit knowledge of the stationary, i.e., the monochromatic, single-particle solution yielding a condition for the balanced beam splitter. This condition is, as was shown, not perfectly met for pulses of finite width. However, given a fixed width of the wave packets and fixed values of T_1 and T_2 , the condition for the balanced beam splitter can be recovered in a trial-and-error fashion by tuning

the two-level system's transition energy or coupling strength such that in a single-photon setup reflection and transmission occur with equal probability. In addition to that, carefully designed and/or tunable dispersion relations such as those available in photonic crystal waveguides [27] can reduce group velocity dispersion over a broad range of carrier wave numbers which makes the beam splitter less dispersive for frequencies of interest.

Alternatively, the Hong-Ou-Mandel interferometry technique could also be exploited to probe the environment by comparison of the measured Hong-Ou-Mandel dip and the “clean” theoretical curve. A numerical fit in which the parameters of the environment are tuned such that the two curves match, finally allows to determine T_1 and/or T_2 times. In that case, however, one still would need sufficient knowledge about possible sources of either T_1 -dissipation or T_2 -dephasing, since these two quantities cannot be clearly separated from one another in the Hong-Ou-Mandel dip.

5. Conclusion and outlook

In conclusion, we analyzed in detail the dynamics of two photons impinging from both ends of a tight-binding waveguide on a local scatterer. This scenario is intimately related to the fundamental Hong-Ou-Mandel effect. Specifically, the joint probability of finding one photon on either side of the impurity after scattering can be calculated numerically in a time-dependent, wave-function-based formalism. As a function of the initial difference in the wave packet separation to the impurity, this quantity is nothing but the famous Hong-Ou-Mandel dip.

In case the local scatterer is just given as an on-site potential, we demonstrated that the Hong-Ou-Mandel effect can become perfect in the sense that the joint probability is zero for maximal wave packet overlap at the scatterer. To this end, we adjusted the parameters of the on-site potential such that a (monochromatic) single photon is reflected and transmitted with equal probability.

We then applied the same strategy to the case of a single two-level system embedded in the waveguide. In this case, we demonstrated that the Hong-Ou-Mandel effect can be less pronounced, i.e., the joint probability is not zero, even though beam splitter imperfections on the single-photon level due to non-zero group velocity dispersion were taken into account. We therefore concluded that an “imperfect” Hong-Ou-Mandel dip can be interpreted as the signature for effective photon–photon interactions which are mediated by the two-level system. In addition, we related our findings to our earlier works [9, 14] in order to get a coherent and complete picture of the dynamics.

We then proceeded by investigating the influence of dissipation and dephasing on the shape of the Hong-Ou-Mandel dip. To this end, we employed a stochastic quantum jump approach and considered the two-level system to be subject to relaxation of T_1 -type as well as pure dephasing of T_2 -type. Due to the normalization of the joint probability to the total probability in the system, T_1 -relaxation only affects the depth of the Hong-Ou-Mandel dip. T_2 -dephasing can also change the offset since the single-photon transmittance is modified. Knowing these properties, Hong-Ou-Mandel interferometry techniques can—at least in principle—also be exploited to probe the environment.

A variety of extensions and modifications to our work presented in this paper can be envisioned for future investigations. For instance, the Hong-Ou-Mandel effect could serve as a probe to identify signatures from more complicated structures such as Jaynes-Cummings cavities, Kerr-nonlinear media, or tunable few-level systems. Especially driven three-level systems might be interesting candidates towards a tunable Hong-Ou-Mandel effect. Besides this, the Hong-Ou-Mandel setup is also worth investigating in the context of polaritons such as those emerging in Jaynes-Cummings-Hubbard systems [28–33] and plasmonic elements [34–36]. Here, due to the mixed nature of the elementary excitations, coincidences can be investigated

beyond the photon–photon sector.

Since—by its very nature—the Hong-Ou-Mandel effect is a two-particle phenomenon, our computational framework [8,9] is perfectly suited and readily applicable to the aforementioned scenarios which are important for and at the heart of of solid-state-based quantum optical devices.

Acknowledgments

We thank Andrew Greentree and Melissa Makin for helpful discussions. P. L. acknowledges financial support by the Karlsruhe House of Young Scientists (KHYS) for his stay abroad at the RMIT University, Melbourne. The Ph.D. education of P. L. is embedded in the Karlsruhe School of Optics and Photonics (KSOP). P. L. and K. B. acknowledge financial support by the DFG within the priority programme SPP 1391 “Ultrafast Nanooptics” (grant BU 1107/7-1). We acknowledge support by the DFG and the Open Access Publishing Fund of the Karlsruhe Institute of Technology.